Seismic Design Parameters Derived from Typical Near-Fault Strong Motions

Longjun Xu[1], Hongzhi Zhang[2], Hao Xu[3], and Lili Xie[4]*

1. Associate Professor, Department of Civil Engineering, Harbin Institute of Technology at Weihai, Weihai 264209, China, * Corresponding Author; email: xulongjun80@163.com
2. Graduate Student, Department of Civil Engineering, Harbin Institute of Technology at Weihai, Weihai 264209, China
3. Graduate Student, Department of Civil Engineering, University of Illinois at Urbana-Champaign
4. Professor, Department of Civil Engineering, Harbin Institute of Technology at Weihai, Weihai 264209, China

Received: 02/08/2012
Accepted: 18/06/2013

ABSTRACT

Based on typical near-fault ground motions, relations between motion pulse amplitudes and periods are utilized to scale the difference of near-fault motions between rock and soil sites. Features of ground motion pseudo-velocity response spectra (PVS), normalized pseudo-velocity spectra (NPVS) and bi-normalized pseudo-velocity spectra (BNPVS) are examined by considering the influence of site conditions. Observations show that, the use of parameters PGV and Tp for the normalization of PVS is applicable. They can effectively reduce the scatter in the response spectra of long period range; ground motion pulse waveforms are affected by local site conditions, BNPVS values of soil sites are larger than those of rock sites at normalized period T/Tv less than about 0.7, while at relative periods larger than 0.7 the reverse is true; spectral peak value of BNPVS at rock sites is significantly higher than that of soil sites. Then, using simple pulses and available predictive relationships for near-fault motions, acceleration response spectra of the near-fault region are developed. The BNPVS are finally used to test the applicability of the established design spectra.

Keywords:
Near-fault ground motion; Pulse; Attenuation relations; Bi-pseudo-velocity spectrum; Design spectrum

1. Introduction

Ground motions in the near-fault zone are potentially affected by wave propagation effects known as directivity. Near-fault motions affected by "forward-directivity" usually exhibit the characteristics of large amplitude and long period velocity pulses [1]. To quantify the special effects of forward-directivity and develop design guidelines, much effort has been devoted to the analysis of the dynamic performance of structures subjected to idealized pulse motions [2-7]. Significant work has also been directed towards developing predictive relationships for parameters that characterize the velocity pulses present in forward-directivity motions [3, 8]. Although those interrelated studies have provided insight on several aspects of near-fault motions and their effects on structures, additional work is needed to capture the nature of forward-directivity motions entirely. For example, previous studies developed predictive relationships for parameters characterizing near-fault motions, but they did not attempt to correlate the simplified pulses to a design spectrum, which is necessary for inclusion in prescriptive building codes.

This paper deals with the special characteristics of forward-directivity motions, using parameter ratios (e.g., AT_v/V, vT_v/D; where A, V and D are peak ground acceleration, velocity and displacement, respectively, and T_v is the pulse period; see Xie et al [9]). The effects of soil condition on forward-

directivity ground motion pulses are analyzed based on a comprehensive study of 53 typical near-fault records. Pseudo-velocity response spectra (PVS), normalized pseudo-velocity spectra (NPVS) and bi-normalized pseudo-velocity spectra (BNPVS) are examined by considering the influence of site conditions. Using simple pulses and available predictive relationships for near-fault motion pulse parameters, acceleration design spectra of the near-fault region is developed. Finally, the BNPVS are used to construct response spectra to test the applicability of the established design spectra.

2. Typical Near-Fault Strong Motions

A dataset of 53 near-fault ground motion records was included in the analysis. These stations together with the earthquake information are listed in Table (1). Near-fault records were selected from the strong

Table 1. Stations included in the analysis of near-fault ground motions (compiled by Bray and Rodriguez-Marek [8]).

Earthquake	Station	Dis. R (km)	Site	PGA (g)	PGV(cm/s)	PGD (cm)	T_v/s	$T_{v\text{-}p}$ /s
Parkfield	Cholame#2	0.1	Soil	0.47	75	22.5	0.67	0.66
	Temblor	9.9	Rock	0.29	17.5	3.17	0.44	0.4
San Fernando	Pacoima Dam	2.8	Rock	1.47	114	29.6	1.44	1.15
Imperial Valley	Brawley Airport	8.5	Soil	0.21	36.1	14.6	2.56	3.11
	EC County Center FF	7.6	Soil	0.22	54.5	38.4	3.78	3.44
	EC Meloland Overpass FF	0.38	Soil	0.38	115	40.2	2.82	2.86
	El Centro Arrar#10	8.6	Soil	0.23	46.9	31.4	3.93	3.82
	El Centro Arrar#3	9.3	Soil	0.27	45.4	17.9	4.5	4.27
	El Centro Arrar#4	4.2	Soil	0.47	77.8	20.7	4.31	4
	El Centro Arrar#5	1	Soil	0.53	91.5	61.9	3.37	3.25
	El Centro Arrar#6	1	Soil	0.44	112	66.5	3.65	3.41
	El Centro Arrar#7	10.6	Soil	0.46	109	45.5	3.73	3.31
	El Centro Arrar#8	3.8	Soil	0.59	51.9	30.8	3.98	4
	El Centro Diff. Array	5.3	Soil	0.44	59.6	38.7	4.18	3.02
	Holtville Post Office	7.5	Soil	0.26	55.1	33	4.28	4.2
	Westmorland Fire Sta	15.1	Soil	0.1	26.7	19.2	3.93	4.71
Morgan Hill	Coyote Lake Dam	0.1	Rock	1	68.7	14.1	0.73	0.71
	Gilroy Array#6	11.8	Rock	0.61	36.5	6.6	1	1.16
Superstition Hill (B)	El Centro Imp. Co. Cent	13.9	Soil	0.31	51.9	22.2	1.85	1.25
	Parachute Test Site	0.7	Soil	0.42	107	50.9	2.11	1.86
Loma Prieta	Gilroy-Gavilan Coll.	11.6	Rock	0.41	30.8	6.5	1.16	0.38
	Gilroy-Historic Bldg.	12.7	Soil	0.29	36.8	10.1	1.33	1.47
	Gilroy Array#1	11.2	Rock	0.44	38.6	7.2	1.16	0.4
	Gilroy Array#2	12.7	Soil	0.41	45.6	12.5	1.36	1.46
	Gilroy Array#3	14.4	Soil	0.53	49.3	11	1.46	0.48
	LGPC	6.1	Rock	0.65	102	37.2	2.14	0.79
	Saratoga-Aloha Ave	13	Soil	0.38	55.5	29.4	2.31	1.55
	Saratoga-W Valley Coll.	13.7	Soil	0.4	71.3	20.1	1.71	1.14
Erzincan, Turkey	Erzincan	2	Soil	0.49	95.5	32.1	2.27	2.23
Landers	Lucerne	1.1	Rock	0.78	147	266.2	5.39	4.3
Northridge	Jensen Filter Plant	6.2	Soil	0.62	104	45.2	1.99	2.86
	LA Dam	2.6	Rock	0.58	77	20.1	1.24	1.3
	Newhall-Fire Sta	7.1	Soil	0.72	120	35.1	0.95	0.71
	Newhall-W. Pico Cyn. Rd	7.1	Soil	0.43	87.7	55.1	2.19	2.03
	Pacoima Dam (Downstr)	8	Rock	0.48	49.9	6.3	0.61	0.44

Table 1. Continue

Earthquake	Station	Dis. R (km)	Site	PGA (g)	PGV (cm/s)	PGD (cm)	T_v/s	$T_{v\text{-}p}$ /s
Northridge	Pacoima Dam (Upper Left)	8	Rock	1.47	107	23	0.89	0.73
	Rinaldi Receiving Sta	7.1	Soil	0.89	173	31.1	1.31	1.06
	Sylmar-Converter Sta	6.2	Soil	0.8	130	54	2.87	1.1
	Sylmar-Converter Sta E.	6.1	Soil	0.84	116	39.4	2.64	2.92
	Sylmar-Olive View FF	6.4	Soil	0.73	123	31.8	1.76	2.42
Kobe	KJMA (Kobe)	0.6	Rock	0.85	96	24.5	1.91	0.86
	Kobe University	0.2	Rock	0.32	42.2	13.1	1.59	1.33
	OSAJ	8.5	Soil	0.08	19.9	9.2	3.83	1.18
	Port Island (0 m)	2.5	Soil	0.38	84.3	45.1	1.91	1.3
Kocaeli	Arcelik	17	Rock	0.21	42.3	44.4	6.82	5.24
	Duzce	12.7	Soil	0.37	52.5	16.4	1.92	1.37
	Gebze	17	Rock	0.26	40.7	39.5	5.04	4.62
Chi-Chi	TCU052	0.2	Soil	0.35	159	105.1	3.14	4.48
	TCU068	1.1	Soil	0.57	295.9	101.4	2.41	4.06
	TCU075	1.5	Soil	0.33	88.3	39.5	2.3	2.03
	TCU101	2.9	Soil	0.2	67.9	75.4	5.35	8.62
	TCU102	1.8	Soil	0.3	112.4	89.2	3.85	2.52
	TCU103	4	Soil	0.13	61.9	87.6	9.52	7.19
Duzce	Bolu	17.6	Soil	0.82	62.1	13.6	0.79	0.57

motion database of the Pacific Earthquake Engineering Research Center (http://peer.berkeley.edu/). These records are restricted to those from shallow earthquakes in active tectonic regions, and the near-fault ground motions obtained are typical forward-directivity records. There are 15 records with magnitude 6.1 to 7.4 on rock sites, and 39 records with magnitude 6.1 to 7.6 at soil sites. Fault distance R is the closest distance to the fault plane. More detailed information of the records and the criteria for site classification and their incorporation into the motion database are given in Bray and Rodriguez-Marek [8].

3. Statistical Results

3.1. Parameter Ratios

The ratios AT_v/V, VT_v/D and $T_{v\text{-}p}/T_v$ of the forward-directivity motions are examined accounting for the influence of local site conditions. The definition of equivalent velocity pulse period T_v uses either the zero crossing time or the time at which velocity is equal to 10% of the peak velocity for this pulse [8]. $T_{v\text{-}p}$ denotes the period with the peak spectral value in a 5%-damped velocity response spectrum.

Relations between the product of A, T_v and V on rock and soil sites are illustrated in Figure (1a). Linear fitting shows that the ratio AT_v/V at rock sites is significantly larger than that of soil sites. These relations show clear difference between motions on rock and soil sites. It is noted that the data at soil sites have larger scatter than those of rock sites, which indicates the great uncertainty in the estimate of AT_v/V. The distribution of AT_v/V with regard to magnitude and site condition is shown in Figure (1b). Initial regression analysis shows that predicted AT_v/V ratio increases with magnitude rising at rock sites, while decreasing with magnitude rising at soil sites. For magnitudes less than 6.7, AT_v/V ratio is higher at soil sites than that of the rock sites; for magnitudes larger than 6.7, the reverse is true. Figure (1c) shows that the VT_v/D ratio at rock sites is appreciably smaller than that of the soil sites. This trend is different from that of the AT_v/V ratio. Specifically, the distribution of the ground motion VT_v/D ratio regarding magnitude and site conditions shown in Figure (1d) indicates a larger VT_v/D at soil sites than at rock sites. This difference decreases as magnitude increases to 7.1. These observations indicate that pulses shapes are affected by both magnitude and local site conditions.

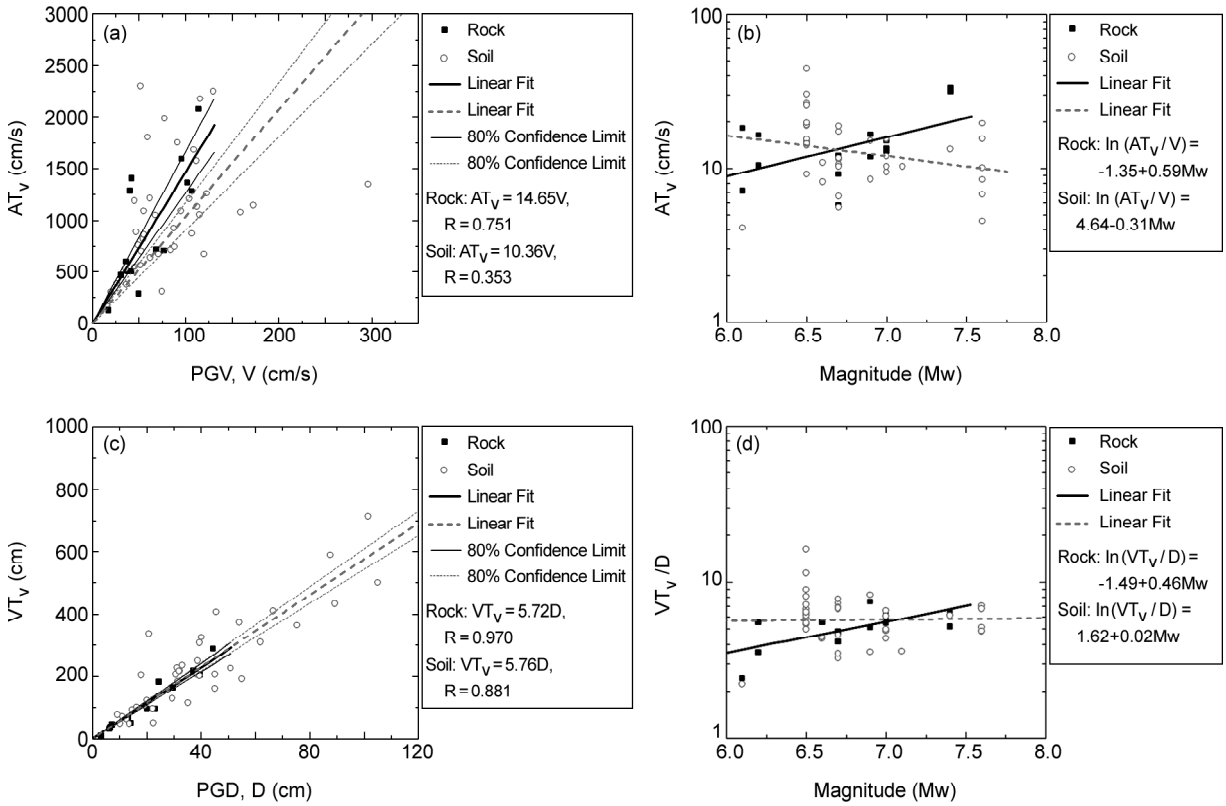

Figure 1. (a) AT_v versus V, (b) variation of ratio ATv/V with Mw, (c) VT_v versus D, and (d) variation of ratio AT_v/V with Mw.

The period corresponding to the peak of the velocity response spectrum ($T_{v\text{-}p}$) and the approximate period of the dominant velocity pulse (T_v) are major parameters in the characterization of near-fault ground motions. Comparisons of $T_{v\text{-}p}$ with T_v for rock and soil sites have been illustrated in Figure (2). Observe that the ratio between $T_{v\text{-}p}$ and T_v exhibits some differences at different site conditions. The ratio of $T_{v\text{-}p}$ to T_v for rock is about 15% less than that for soil sites. The discrepancies of the period ratios for different site conditions are deemed pulse waveform dependent.

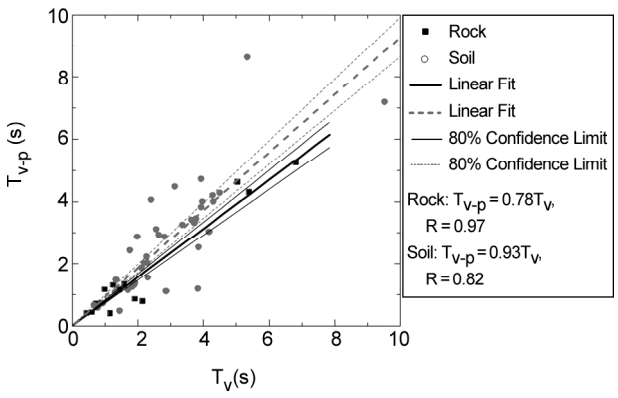

Figure 2. Comparison of $T_{v\text{-}p}$ with T_v.

3.2. Response Spectra

Figure (3a) illustrates the pseudo-velocity spectra (PVS) of the selected near-fault motions corresponding to soil sites, rock sites and both, respectively. These figures reveal that spectral ordinates of near-fault records vary significantly, especially at the long period range. The peak amplitudes and predominate periods are also characterized by large dispersion. Figure (3b) displays the normalized pseudo-velocity response spectra (NPVS) of these motions. This normalization effectively reduces the dispersion of PVS, which makes NPVS more regular, especially for spectral values near peak and at long period range. If we further normalize the period axis of the NPVS with respect to their corresponding T_p values, the BNPVS as shown in Figure (3c) are obtained. Inspection of Figure (3c) exhibits that they are characterized by a small variation of normalized peak spectral amplitudes particularly in a relative long period range.

To differentiate the response spectra between soil and rock sites, these three types of spectra are averaged according to site conditions, respectively, as illustrated in Figure (4). Mean PVS and NPVS for both kinds of site conditions exhibit similar

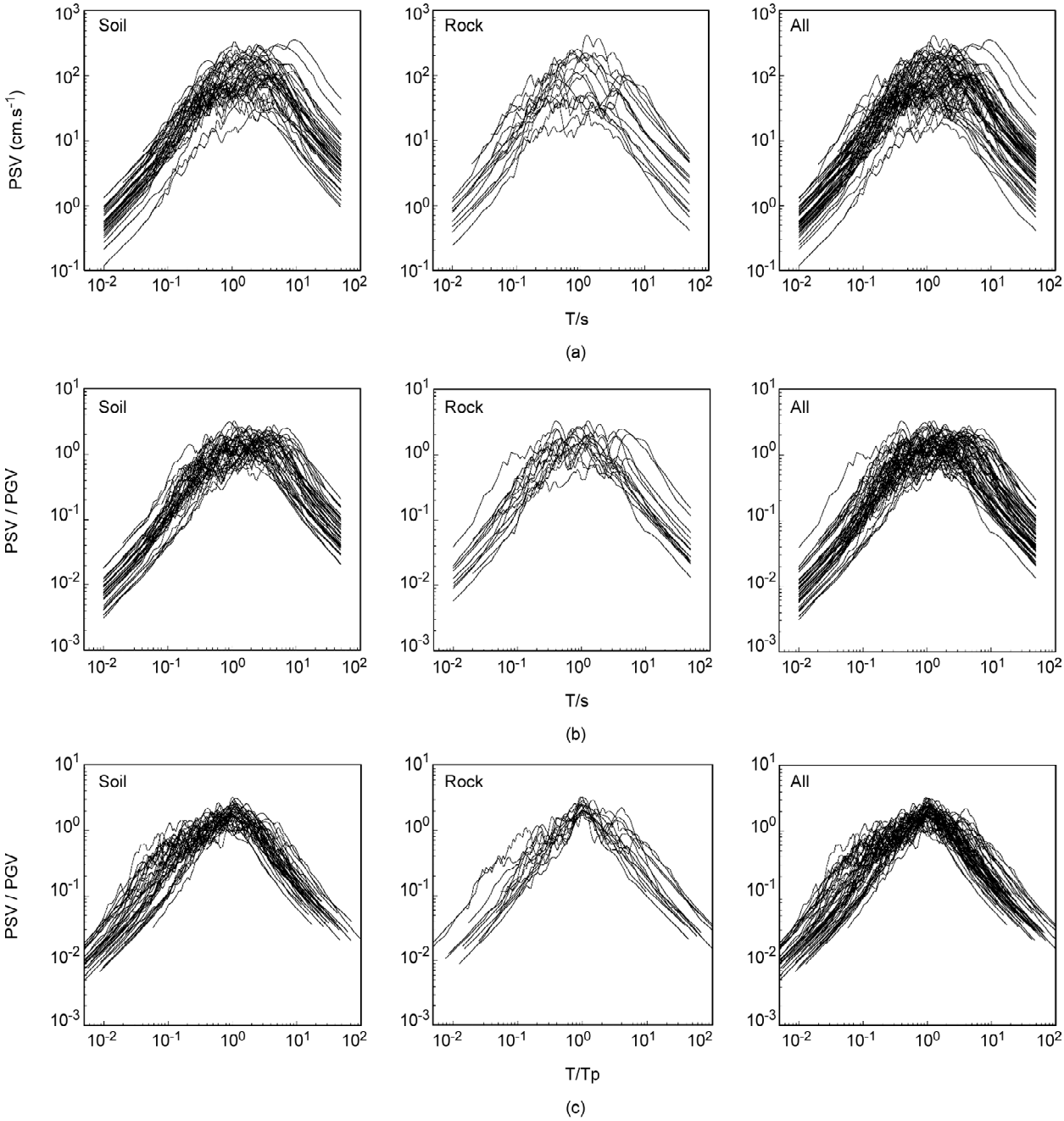

Figure 3. Three types of response spectra for near-fault forward-directivity ground motions (5% damping).

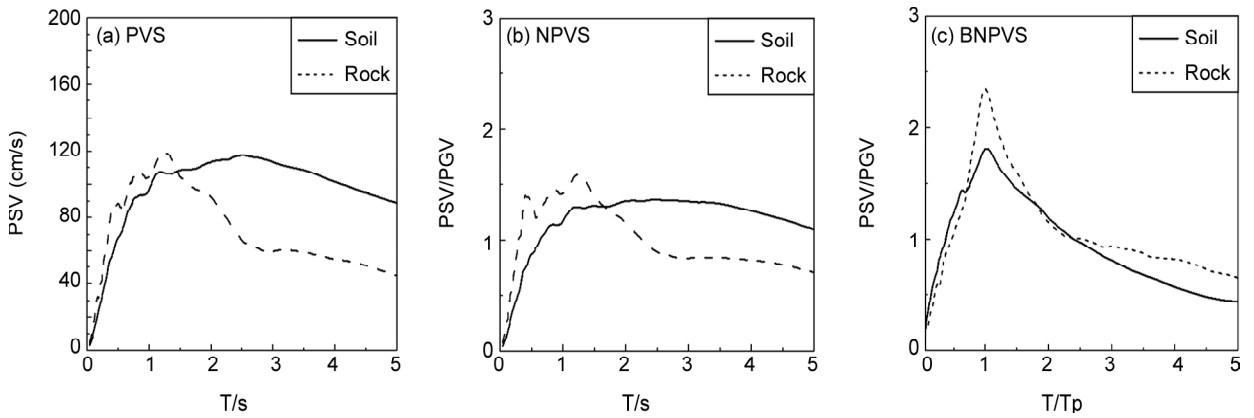

Figure 4. Mean curves of three types of response spectra considering the effect of site condition.

features. Mean spectral ordinates for soil sites are lower than those of rock sites at short period range, while at long periods the reverse is true. For mean BNPVS, spectral ordinates for soil sites are higher than those of rock sites at normalized period T/T_v less than about 0.7, while at relative periods larger than 0.7 the reverse seems true. An important aspect is seen that spectral peak value of rock sites is significantly larger than that of soil sites. These observations indicate that BNPVS has more salient features than other spectra on reflecting the difference between soil and rock sites. Figure (5a) and (5b) display 5% damped mean and mean+1std curves of BNPVS at soil and rock sites, respectively. To quantify the dispersion for different types of response spectra, Figure (5c) illustrates the coefficient of variation (COV) of these spectra corresponding to all the ground motions considered (the abscissa axis of BNPVS has multiplied the mean predominate period of NPVS of all the records). It is evident that dispersion of BNPVS is the lowest, particularly at the long period range. Thus, the parameters V and Tp, which are used for the normalization of pseudo velocity response spectra, can effectively normalize the response spectra and reduce the scatter of actual near-fault records.

4. Characterization of Simplified Pulses

In this section, we will check whether simplified pulses with different waveforms are able to provide an interpretation for the observed phenomenon of actual near-fault directivity ground motions.

Table (2) illustrates four sets of pulses including acceleration, velocity and displacement time series, which have been commonly used as representation for the effect of forward-directivity of the near-fault motions. Each pulse can be fully determined by two parameters: the velocity pulse period T_v and acceleration pulse amplitude A. Based on the parameters T_v and A, pulse amplitude V(PGV) and D (PGD) can be derived, and as a consequence, ratios of $AT_v/V$and VT_v/Dthat reveal the relationship between pulse amplitudes and period can be obtained. Ratios of AT_v/V and VT_v/D for these four pulses have been listed in Table (3). The AT_v/Vratios for the four pulses are significantly different. FDP4 has a largest AT_v/Vratio of 12, while FDP1 has a smallest ratio of four. However, unlike AT_v/V, the ratio VT_v/D decreases gently as the pulses change orderly from FDP1 to FDP4. For the comparison, 5% damped

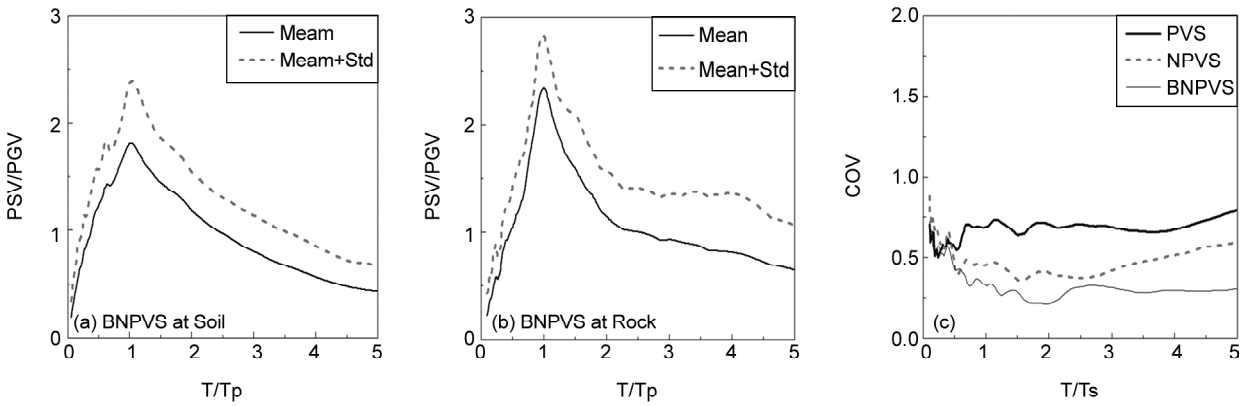

Figure 5. Mean and mean+1std curves of BNPVS at (a) soil and (b) rock sites, and (c) COVs of three kinds of response spectra.

Table 2. Description and classification of the simple pulses.

Pulses		1. Rec (FDP1)	2. Half-sin (FDP2)	3. Tri (FDP3)	4. Qua (FDP4)
Forward-Directivity Pulse (FDP)	Acceleration	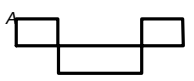		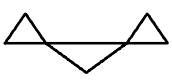	
	Velocity	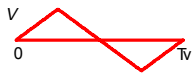			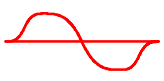
	Displacement	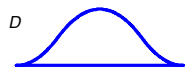	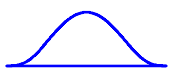		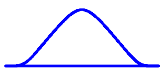

Table 3. Some parameter ratios and response spectral peak amplifications.

Pulse	1. Rec (FDP1)	2. Half-sin (FDP2)	3. Tri (FDP3)	4. Qua (FDP4)
AT_v/V	4.00	6.28	8.00	12.00
VT_v/D	4.00	3.52	3.43	3.20
$T_{v\text{-}p}/T_v$	0.98	0.92	0.90	0.87
β_{BNPVS}	2.12	2.52	2.59	2.82

velocity response spectra of these pulses are calculated; parameter ratio of the period corresponding to the velocity spectral peak value to the pulse period ($T_{v\text{-}p}/T_v$) is examined and listed in Table (3). The ratio of $T_{v\text{-}p}/T_v$ clearly depends on the basic pulses of the equivalent pulses, and it decreases when the shape of the basic pulse becomes sharper. For further comparison, Figure (6a) gives the plotted PVS for four pulses (assuming that four pulses have equal acceleration amplitude A and pulse duration T_v of 1 g and 1 s, respectively). The normalized pseudo-velocity response spectra (NPVS) for the four pulses are drawn in Figure (6b). It shows that the NPVS becomes more regular than PVS when the influence of pulse intensity (V) is removed. Figure (6c) illustrates the BNPVS for four pulses considered. It is evident that BNPVS for four pulses are also in good accordance with each other. While it is noted that with equal acceleration amplitude A and pulse duration T_v, the PVS and BNPVS can reflect certain different features, ordinates of PVS decrease with the pulse waveform getting sharp (from FDP1 to FDP4). For BNPVS, spectral values increase at relative periods T/T_v larger than about 0.6 when pulse changes orderly from FDP1 to FDP4, and spectral ordinates decrease at $T/T_v<0.6$ when pulse waveform becomes sharp. The peak amplification of BNPVS for FDP1, FDP2, FDP3 and FDP4 are 2.12, 2.52, 2.59 and 2.82, respectively, see Table (4).

Parameter ratios AT_v/V, VT_v/D, $T_{v\text{-}p}/T_v$ and spectral peak value BNPVS presented are introduced to identify the waveforms of simplified pulse-type motions. Above analysis indicates that ground motion pulse of rock sites is sharper than that of the soil sites, they are pulse shape-dependent and highlight the need to consider the waveform in choosing equivalent pulse in the near-fault region.

As it is known, the velocity amplitude V heavily depends upon its predecessor acceleration pulse. The amplitude, duration and sharpness of the dominant acceleration pulse may have contributed to the differences in measured AT_v/V ratio of the near-fault

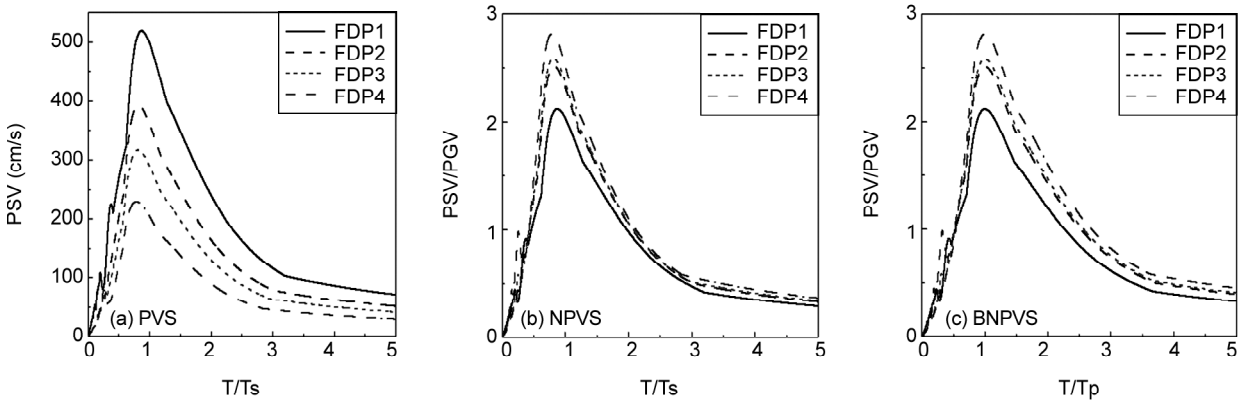

Figure 6. Mean curves of three types of response spectra considering the effect of site condition.

Table 4. Coefficients for estimated near-fault response spectra.

Coeff.	α_{M6} (g)				β_a ($\beta_{a\text{-}p}$)				R_a ($T_{a\text{-}p}/T_v$)				T_{M6} (s)	r
	FDP1	FDP2	FDP3	FDP4	FDP1	FDP2	FDP3	FDP4	FDP1	FDP2	FDP3	FDP4		
Rock	A_{M6}	A_{M6}	A_{M6}	A_{M6}	4.19	3.35	2.74	2.04	0.75	0.70	0.69	0.68	0.51	0.75
Soil	A_{M6}	A_{M6}	A_{M6}	A_{M6}									0.98	0.65

motions. The observations summarized in Figure (1) are likely a result of both longer site periods of soil sites than at rock sites, and nonlinearity. The longer site periods of soil sites imply that velocity is likely to have larger amplification than acceleration (due to site effects) as the magnitude of the earthquake (hence the site period) increases. For this reason, the decreasing trend in AT_v/V is observed for soil sites. For rock sites, increases in A and V with magnitude are likely to be proportional and the increasing trend of AT_v/V for rock sites could be attributed to the increase of T_v with magnitude. Soil nonlinearity enhances these effects and it affects ground shaking via the strains induced in the soil. In the near-fault zone, larger ground motions generate larger strains in the soil, which results in a reduction in soil shear stiffness and an increase in soil damping. The reduction in shear stiffness causes an increase in site period and enhances the pulse duration; the increase in soil damping can dramatically reduce the wave amplitude, particularly of acceleration pulse (A). On the other hand, the effect of the soil layer is generally to increase both the pulse peak velocity V and the period of the input motion. The amount of the increase depends on the level of the input ground motion, the thickness and physical properties of the soil layer [10]. Consequently, as the intensity of the pulses increases with earthquake magnitude, the AT_v/V ratio of soil sites decreases and becomes lower than that of rock sites.

5. Derivations from Forward-Directivity Ground Motions

5.1. Response Spectra Regarding Simple Pulses

Previous analysis has shown that ratios of AT_v/V, VT_v/D and $T_{v\text{-}p}/T_v$ of near-fault ground motions are site-dependent, at least qualitatively. The objective of this section is, first, to estimate equivalent acceleration amplitude A_e with well-calibrated regression relations and the simple pulse waveforms illustrated in Table (1), and subsequently, to consider their integration in developing applicable design spectra in the near-fault region.

To estimate the equivalent acceleration amplitude A_e that controls the velocity pulse of these special motions, a simple way is to associate it with velocity amplitude V and pulse period T_v of recorded ground motions. In the absence of more general studies, we used the relationships proposed by Bray and Rodriguez-Marek [10] that correlate V and T_v with site conditions and magnitude for forward-directivity ground motions. These relationships are:

$$\begin{aligned} \ln(V_r) &= 4.46 + 0.34M_w - 0.58\ln(R^2+49) \\ \ln(V_s) &= 4.58 + 0.34M_w - 0.58\ln(R^2+49) \end{aligned} \quad (1)$$

$$\begin{aligned} \ln(T_{v.r}) &= -8.60 + 1.32M_w \\ \ln(T_{v.s}) &= -5.60 + 0.93M_w \end{aligned} \quad (2)$$

To see the possible results derived from Eqs. (1) and (2), simplified pulse waveforms for forward-directivity motions are assumed to match the near-fault directivity motions, respectively. Thus the equivalent acceleration amplitude A_e of these special motions can be estimated through the determinate relationships between A, V and T_v of the simple pulses considered.

The estimated Ae with respect to site conditions and magnitude for forward-directivity motions are illustrated in Figure (7). An interesting phenomenon is that the equivalent acceleration amplitude Ae derived decreases with the magnitude increasing.

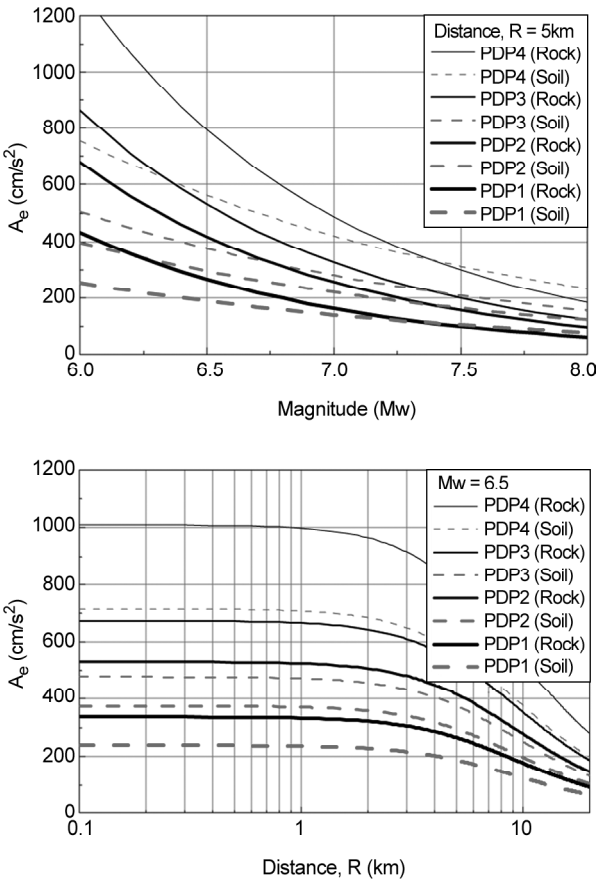

Figure 7. Estimated A_e for forward-directivity ground motion pulses.

For magnitude less than about 7.4, the derived A_e at rock sites are higher than those at soil sites are, whereas for magnitude larger than 7.4, estimated A_e at rock are lower than those at soil are, and almost independent on soil conditions. These derivations are quite different from those of predicted PGA of ordinary near-field ground motions, which show distinct dependence of PGA with site conditions, and that PGA increases with the increasing of earthquake magnitude and/or with the site soil getting soft.

A simple way of estimating the response spectra of pulse-type motions in the near-fault region is to associate the simple pulse motions with the derived equivalent acceleration A_e. For each pulse considered, a response spectrum curve can be drawn by plotting the peaks of response spectra for different pulses with a determinate magnitude. Unlike the conventional ground motion response spectra, the plotted spectral ordinates at shorter period range are related to smaller earthquakes, and to larger events at a longer period range. Assume that the derived pulse acceleration (A_{M6}) and the peak period ($T_{M6} \cdot R_a$) of response spectrum for $Mw=6$ are equal to the seismic coefficient α_m and characteristic period T_g, respectively; and T_0 is given by T_g / 4, then the near-fault response spectra can be given by [11]:

$$Sa_{NF} = \begin{cases} \left(1 + \dfrac{4(\beta_a - 1)T}{T_{M6} \times R_a}\right) \times \alpha_{M6} \\ \beta_a \times \alpha_{M6} \\ \beta_a \left(\dfrac{T}{T_{M6} \times R_a}\right)^{-\gamma} \times \alpha_{M6} \end{cases} \quad (3)$$

$$0 \le T < 0.25 T_{M6} \cdot R_a$$

$$0.25 T_{M6} \cdot R_a \le T < T_{M6} \cdot R_a$$

$$T_{M6} \cdot R_a \le T < 6s$$

where some of the coefficients for the near-fault spectra in terms of pulses are listed in Table (4). The derived spectra at rock and soil sites with fault distance R = 5 and 10 km are plotted in Figure (8). Note that, fault distance significantly affects spectral ordinates; spectral values decrease as the distance increases. However, soil conditions can slightly influence the near-fault spectra at periods larger than characteristic period T_g, and at periods less than T_g,

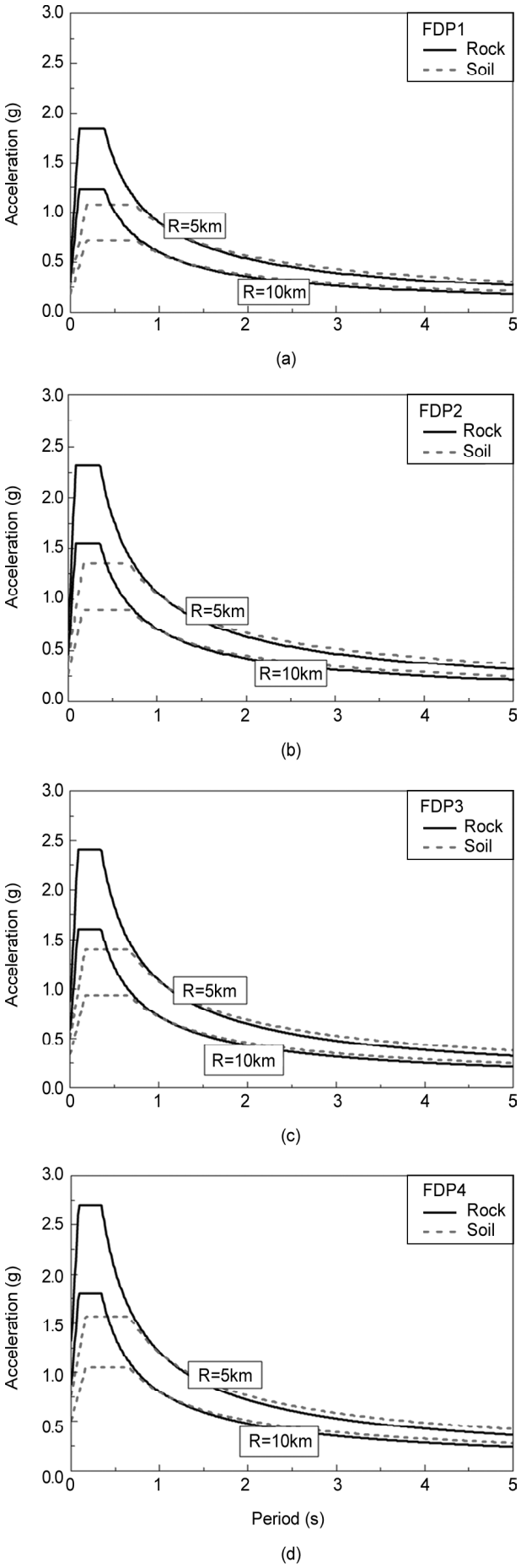

Figure 8. Estimated spectra based on simple pulses.

spectra at rock are significantly higher than the ones at soil sites.

A comparison among these near-fault spectra for the four pulses is shown in Figure (9). It is observed that fault spectra derived from four pulses exhibit evident differences. FDP1-based spectra are significantly lower than those derived from the other pulses, while the differences between spectra estimated based on FDP2, FDP3 and FDP4 are small at periods larger than period T_g. Another significant discrepancy restricts to periods less than T_g, where the spectral ordinates increase as the pulse shape becomes sharp. These observations indicate that local site conditions can only heavily affect pulse-type ground motions and their response spectra of smaller earthquakes, while for larger earthquakes the influence of site conditions is not distinct in the near-fault zone.

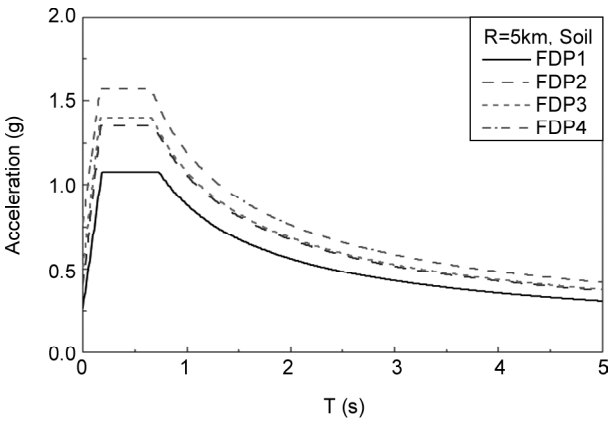

Figure 9. Comparison of the design spectra based on different simple pulses [11].

5.2. Response Spectra Regarding BNPVS of Actual Motions

Based on statistical result shown in Figure (5), relationships between Eqs. (1) and (2), and noting that T_p and T_v have relationships [11]:

$$\begin{cases} T_{p,\,rock} = 0.78 T_{v,\,rock} \\ T_{p,\,soil} = 0.93 T_{v,\,soil} \end{cases} \tag{4}$$

the pseudo-velocity response spectra can be constructed by linking all peaks of the PVS (84.1th percentile) with different earthquake magnitudes. We assume that the derived pseudo-velocity (V_{M6}) and the peak period (T_p) of response spectrum for $Mw = 6$ are equal to the seismic coefficient V_m and characteristic period T_g, respectively; and the corner period T_0 is empirically given by $T_g/4$, then the derived near-fault pseudo-acceleration response spectra ($S_{p\text{-}a}$) can be given by:

$$S_{p-a} = \begin{cases} \left[1 + (\beta_{p-v} - 1) \times \dfrac{T}{T_0}\right] \times \alpha_m \\ \beta_{p-v} \times \alpha_m \\ \beta_{p-v} \times \left(\dfrac{T}{T_g}\right)^{-\gamma} \times \alpha_m \end{cases} \tag{5}$$

$$0 \le T < 0.25 T_g$$

$$0.25 T_g \le T < T_g$$

$$T_g \le T$$

where α_m is the design pseudo-acceleration, which is obtained by transforming pseudo-velocity spectra to pseudo-acceleration spectra; $\beta_{p\text{-}v}$ is the peak value of mean+1std spectra in Figure (5); r is the exponent in spectra long period range. The values of coefficients in Eq. (5) are listed in Table (5). The derived spectra at rock and soil sites with fault distance $R = 5$ km are plotted in Figure (10a). Note that, site condition significantly affects spectral ordinates. Spectral values at rock sites are higher than those of the soil sites, and the difference decreases when the spectral periods become larger than characteristic period T_g. This observation indicates that buildings on rock sites can be even more dangerous than those on soil sites, particularly for ordinary buildings with short to medium vibration periods. Design spectral amplifications are drawn in Figure (10b), which show that amplification values at rock sites are significantly higher than those at soil sites at periods less than about 0.5 s, and the reverse is true when periods are larger than 0.5 s.

Examples of the comparisons among the derived spectra based on simple pulses and on BNPVS have been shown in Figure (11). It is observed that, at rock

Table 5. Coefficients for pseudo-acceleration design spectra (5% damping, R=5km).

Site Conditions	α_m /g	$\beta_{p\text{-}v}$	T_g /s	r
Rock	0.89	2.83	0.40	0.75
Soil	0.43	2.37	0.91	0.65

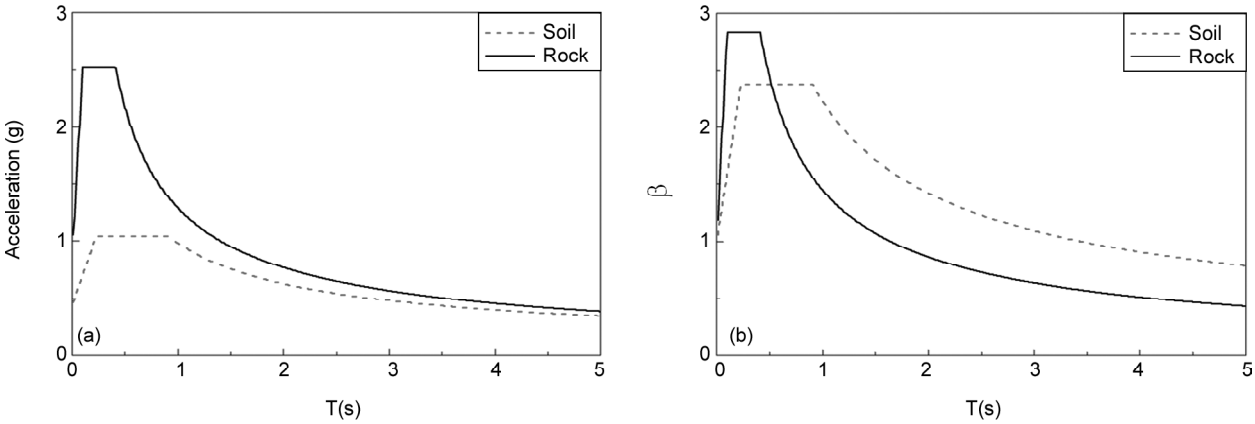

Figure 10. Derived spectra based on BNPVS (R=5km).

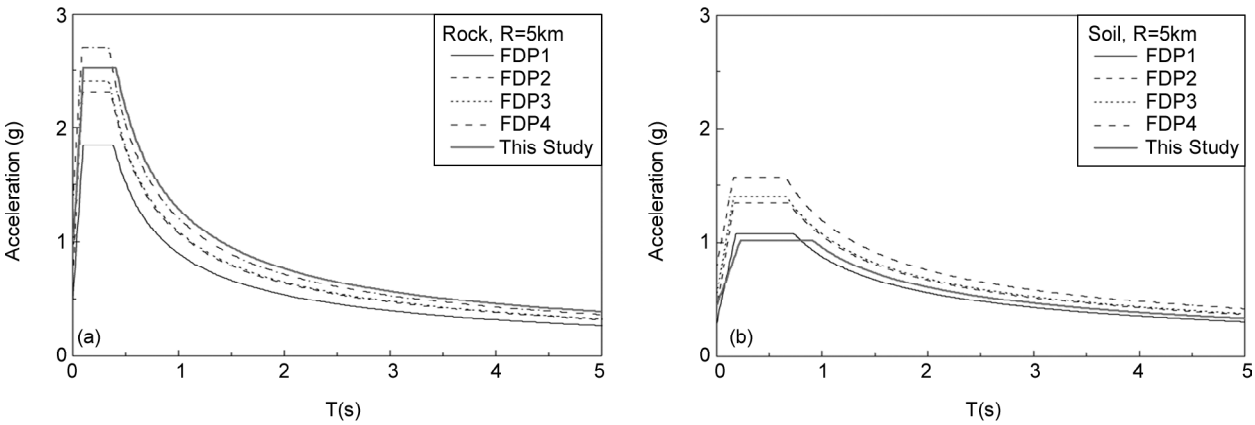

Figure 11. Comparisons of design spectra with spectra proposed by Xu et al [11].

sites, derived spectrum based on BPPVS agrees well with spectrum for pulse FDP3 at periods less than T_g, while it approaches more to FDP4-based spectrum at periods larger than T_g. For spectra at soil sites, the BNPVS-based spectrum agrees well with FDP1-based spectrum and is much lower than expected.

6. Conclusions

This investigation of the parameter ratios and response spectra of typical forward-directivity strong motions and simple pulses led to the following findings:

- Ratios AT_v/V and $T_{v\text{-}p}/T_v$ for near-fault, forward-directivity ground motions are substantially affected by local site conditions. AT_v/V ratio is clearly larger at rock sites than that at soil sites, while the VT_v/D and $T_{v\text{-}p}/T_v$ ratios are smaller at rock sites than these at soil sites for earthquake magnitudes lower than about Mw = 7.0.
- The use of parameters V and T_p for the normalization of pseudo-velocity response spectra can effectively reduce the scatter, in particular for the response spectra at the long period range.
- BNPVS values at soil sites are larger than those at rock sites at normalized period T/T_v less than about 0.7, while the reverse is true at relative periods larger than 0.7; spectral peak value of BNPVS at rock sites is significantly higher than that at soil sites.
- Parameters and ratios of AT_v/V, VT_v/D, $T_{v\text{-}p}/T_v$ and $\beta_{v\text{-}p}$ for four simplified pulses (rectangular, half-sine, triangular and quadratic) can be significantly different due to the sharp and flat shape of the acceleration pulses.
- Design spectra are constructed based on simple pulses and on site-dependent BNPVS, respectively. Comparisons of the derived spectra show that site conditions can heavily affect ground motions, and ordinary buildings with short to medium periods on rock sites can be even more dangerous than those on soil sites are.

Acknowledgements

The research summarized in this paper was supported by the Special Fund for Earthquake Scientific Research in the Public Interest (201208013), the National Natural Science Foundation of China (51178152, 50808168), who are gratefully acknowledged.

References

1. Somerville, P.G., Smith, N.F., Graves, R.W., and Abrahamson, N.A. (1997). Modification of Empirical Strong Ground Motion Attenuation Relations to Include the Amplitude and Duration Effects of Rupture Directivity, *Seismological Research Letters*, **68**(1), 199-222.
2. Hall, J.F., Heaton, T.H., Halling, M.W., and Wald, D.J. (1995). Near-Source Ground Motions and Its Effects on Flexible Buildings, *Earthquake Spectra*, **11**(4), 569-605.
3. Alavi, B. and Krawinkler, H. (2000). Considerations of Near-Fault Ground Motion Effects in Seismic Design, *Proceedings of the 12th World Conference on Earthquake Engineering*, New Zealand, Paper No.: 2665.
4. Alavi, B. and Krawinkler, H. (2004). Behavior of Moment-Resisting Frame Structures Subjected to Near-Fault Ground Motions, *Earthquake Engineering and Structural Dynamics*, **33**, 687-706.
5. Sasani, M. and Bertero, V.V. (2000). Importance of Severe Pulse-Type Ground Motions in Performance-Based Engineering: Historical and Critical Review, *Proceedings of the 12th World Conf. on Earthquake Engineering, Auckland*, New Zealand, paper No. 1302.
6. Mavroeidis, G.P. and Papageorgiou, A.S. (2003). A Mathematical Representation of Near-Fault Ground Motions, Bulletin of the Seismological Society of America, **93**(3), 1999-1131.
7. Mavroeidis, G.P., Dong, G., and Papageorgiou, A.S. (2004). Near-Fault Ground Motions, and the Response of Elastic and Inelastic Single-Degree-of-Freedom (SDOF) Systems, *Earthquake Engineering and Structural Dynamics*, **33**, 1023-1049.
8. Bray, J.D. and Rodriguez-Marek, A. (2004). Characterization of Forward-Directivity Ground Motions in the Near-Fault Region, *Soil Dynamics and Earthquake Engineering*, **24**, 815-828.
9. Xie, L., Xu, L., and Rodriguez-Marek, A. (2005), Representation of Near-Fault Pulse-Type Ground Motions, *Earthquake Engineering and Engineering Vibration*, **4**(2), 191-199.
10. Rodriguez-Marek, A. (2000). Near Fault Seismic Site Response, Ph.D. Thesis, Civil Engineering, University of California, Berkeley.
11. Xu, L.J., Rodriguez-Marek, A., and Xie, L.L. (2006). Design Spectra Including Effect of Rupture-Directivity in Near-Fault Region, Earthquake Engineering and Engineering Vibration, **5**(2), 159-170.